

³ Li, C. P., "Time-Dependent Solutions of Nonequilibrium Airflow Past a Blunt Body," *Journal of Spacecraft and Rockets*, Vol. 9, No. 8, Aug. 1972, pp. 571-572.

⁴ Rakich, J. V. and Park, C., "Nonequilibrium Three-Dimensional Supersonic Flow Computations with Application to the Space Shuttle Orbiter Design," Symposium on Application of Computers to Fluid Dynamic Analysis and Design, Polytechnic Institute of Brooklyn, Farmingdale, N.Y., Jan. 1973.

⁵ Anderson, J. D., "A Time-Dependent Analysis for Vibrational and Chemical Nonequilibrium Nozzle Flows," *AIAA Journal*, Vol. 8, No. 3, March 1970, pp. 545-550.

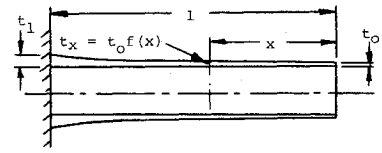
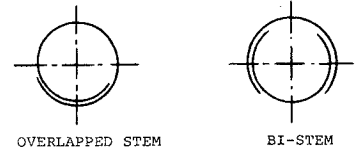


Fig. 1 A thickness tapered boom and examples of open section booms.

a) THICKNESS TAPERED BOOM



b) EXAMPLES OF OPEN SECTION BOOMS

Analysis of Thickness Tapered Booms for Space Applications

RAJNISH KUMAR* AND SHABEER AHMED†

Spar Aerospace Products Ltd., Toronto, Canada

Nomenclature

- A_x, A_o = Transverse accelerations as experienced at x and the tip, in./sec²
 $f(x)$ = Function of x corresponding to thickness profile
 S_{1x}, S_{2x} = Bending stresses for constant and linearly varying accelerations (expressed as % values of uniform boom of thickness t_1)
 S_1, S_2 = Maximum values of S_{1x} and S_{2x}
 t_o, t_1, t_x = Wall thickness at tip, root and x , in.
 T = Thickness parameter = $(t_1/t_o) - 1$
 W_R = Mass ratio, i.e., boom mass expressed as percentage of the mass of a boom of uniform thickness t_1
 x = Dimensionless distance (= distance from the tip divided by the boom length)
 δ_1, δ_2 = Tip deflections (expressed as percentage of the values of a uniform boom of thickness t_1) corresponding to uniform and linearly varying accelerations

Introduction

SPACE booms are usually in the form of thin-walled open section tubes called STEMS¹ (Storable Tubular Extendible Members). Such a boom is stored on a cassette during critical periods of the flight such as launch and deployed in orbit. In the fully deployed position the loads experienced by a boom are mainly inertial loads due to orbital maneuvers. In general the boom experiences constant and/or linearly varying transverse accelerations along the length. Centrifugal action of a spinning spacecraft also causes transverse loads if the boom is not mounted perpendicular to the spin axis. In all these cases the loading at any point will be directly proportional to the mass outboard to that point. Since the boom under such loads acts like a cantilever beam, it suggests that providing a taper on the wall thickness can be an effective way of achieving both a low weight and an improved functional performance of the boom. The description including design and flight experience of tubular booms used for various space applications is given in Ref. 2.

The purpose of this investigation is to analyze the advantages of thickness tapered booms in terms of reductions in weight, stress and the tip deflection, especially when they are used as

antennas.‡ Deflections should be minimized for improved performance of antennas. Examples of open section booms and schematic diagram of a thickness tapered boom are given in Fig. 1. Thickness variation can be obtained by a chemical etching process or by nesting several boom elements to different lengths. Two practically feasible profiles corresponding to linear and parabolic variation of the thickness along the length have been analyzed. This Note is intended for design purposes.

Analysis

For thin walled booms, the mean diameter can be assumed constant along the length as the wall thickness at any section is very small compared to the diameter. Considering the thickness profile as shown in Fig. 1a, the bending stiffness at any section x is directly proportional to t_x . The boom mass can be expressed as follows:

$$W_R = (100t_o/t_1) \int_0^1 f(x) dx \quad (1)$$

For minimum weight objective and practical consideration $t'_x \geq 0$ for $0 \leq x \leq 1$ ($'$ denotes differentiation with respect to x).

If the loading is due to transverse acceleration A_o constant through the length, using the simple beam bending theory, tip deflection and stress developed at any section can be expressed as follows:

$$\delta_1 = 800 \int_0^1 [G(x) - \int_0^x G(x) \cdot dx] \cdot dx \quad (2)$$

$$S_{1x} = 200 \cdot G(x) \quad (3)$$

where

$$G(x) = \left[\int_0^x \int_0^x f(x) \cdot dx \cdot dx \right] / f(x)$$

If the loading is caused by a linearly varying acceleration expressed as $A_x = A_o(1-x)$, the following relations can be obtained for bending stress and tip deflection

$$S_{2x} = 300 \cdot G_1(x) \quad (4)$$

$$\delta_2 = (1200/11) \int_0^1 \left[G_1(x) - \int_0^x G_1(x) \cdot dx \right] \cdot dx \quad (5)$$

where

$$G_1(x) = G(x) - \left[\int_0^x \int_0^x x \cdot f(x) \cdot dx \cdot dx \right] / f(x)$$

Equations 1-5 can be used to determine the effectiveness of any thickness tapered boom when subjected to inertial loading. Linear and parabolic thickness profiles have been evaluated using these relations.

‡ Like the Gemini recovery antenna and Apollo 17 high frequency sounder antennas, etc.

Received July 30, 1973; revision received September 13, 1973.

Index category: Spacecraft Configurational and Structural Design (Including Loads).

* Senior Structural and Dynamics Engineer.

† Space Mechanics Section, Communications Research Center, Ottawa, Canada. Member AIAA.

Linear Thickness Variation

For linear thickness profile $f(x) = 1 + T \cdot x$. The values of maximum bending stress and tip deflection for constant and linearly varying accelerations, and boom mass are as follows:

$$S_1 = (100/3) \cdot (3+T)/(1+T) \quad (6)$$

$$S_2 = 25 \cdot (4+T)/(1+T) \quad (7)$$

$$\delta_1 = \frac{400}{3} \left[\frac{1}{4} + \frac{2}{3T} - \frac{1}{T^2} + \frac{2}{T^3} - \frac{2}{T^4} \cdot \log_e(1+T) \right] \quad (8)$$

$$\delta_2 = \frac{1000}{11} \left[\frac{3}{10} + \frac{13}{12T} - \frac{5}{3T^2} + \frac{7}{2T^3} + \frac{1}{T^4} - \frac{1}{T^4} \left(4 + \frac{1}{T} \right) \cdot \log_e(1+T) \right] \quad (9)$$

$$W_R = 50 \cdot (2+T)/(1+T) \quad (10)$$

The maximum stress values occur at the root. It can be seen that as $T \rightarrow \infty$, $S_1 \rightarrow 33.3\%$, $S_2 \rightarrow 25\%$, $\delta_1 \rightarrow 33.3\%$, $\delta_2 \rightarrow 27.3\%$, and $W_R \rightarrow 50\%$.

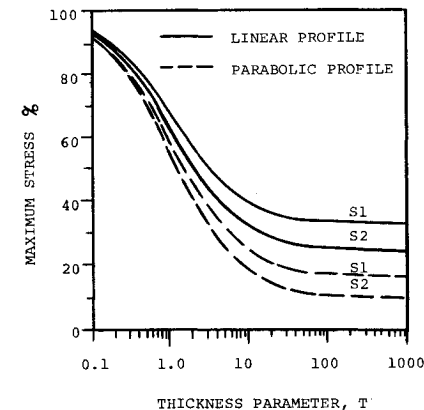
Parabolic Thickness Variation

Parabolic profile which minimizes the maximum bending stress and tip deflection under inertial loading is $f(x) = 1 + T \cdot x^2$. The values of tip deflections, maximum bending stresses which occur at the root and boom mass are as follows:

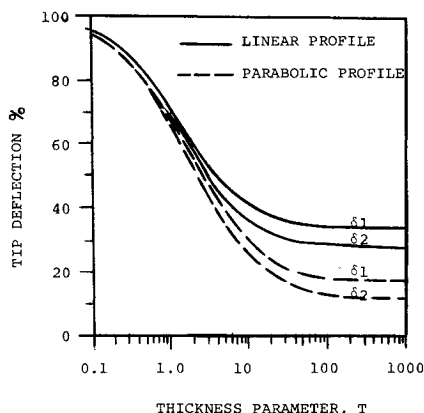
$$S_1 = (50/3) \cdot (6+T)/(1+T) \quad (11)$$

$$S_2 = 10 \cdot (10+T)/(1+T) \quad (12)$$

$$\delta_1 = \frac{200}{3} \left[\frac{1}{4} + \frac{5}{2T} - \frac{5}{T^2} \log_e(1+T)^{1/2} \right] \quad (13)$$



a) MAXIMUM BENDING STRESS



b) TIP DEFLECTION

Fig. 2 Maximum bending stress and tip deflection due to inertial loads corresponding to constant and linearly varying transverse accelerations.

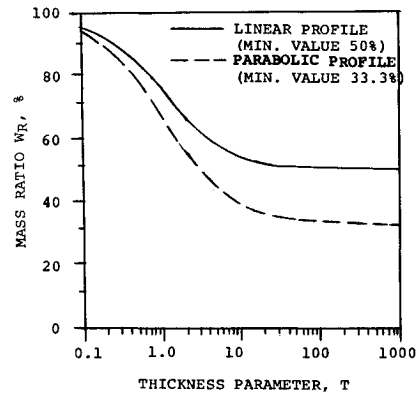


Fig. 3 Mass of boom for different thickness profiles.

$$\delta_2 = \frac{200}{11} \left[\frac{13}{20} + \frac{61}{6T} + \frac{7}{T^2} - \frac{25}{T^2} \log_e(1+T)^{1/2} - 7T^{-5/2} \cdot \tan^{-1} T^{1/2} \right] \quad (14)$$

$$W_R = (100/3) \cdot (3+T)/(1+T) \quad (15)$$

As

$T \rightarrow \infty$, $S_1 \rightarrow 16.7\%$, $S_2 \rightarrow 10\%$, $\delta_1 \rightarrow 16.7\%$, $\delta_2 \rightarrow 11.8\%$ and

$$W_R \rightarrow 33.3\%$$

Using numerical analysis techniques, higher degree polynomial profiles can also be evaluated for their effectiveness in reducing tip deflection, stresses and weight. However, considering a cubic polynomial profile, it was found that the advantages of adopting a higher degree polynomial profiles than parabolic are marginal.

Results and Discussions

Advantages of a thickness tapered boom over a uniformly thick boom in terms of reductions in weight, maximum stresses and tip deflections can be determined by using Eqs. 1-5. For linear and parabolic thickness variations, maximum bending stresses occur at the root. Figure 2a gives the maximum bending stresses for the two profiles as a percentage of the value of a uniformly thick boom. Figure 2b gives the tip deflection as a function of the thickness parameter T . It can be observed that as the thickness parameter T is increased, maximum stresses and tip deflection reduce to constant values. In addition to reducing maximum stress and deflection values, each profile results in considerable weight saving as shown in Fig. 3.

Figures 2 and 3 indicate that improvements in the stress, deflection and weight values are most significant as T is increased from 0 to 10, small for T between 10 and 100 and negligible for T greater than 100. Ignoring the complexity of producing a thickness taper, the parabolic profile has better performance than linear thickness profile under inertial loads. However, it has been estimated that the advantage of adopting a higher degree polynomial profile than parabolic will be marginal.

From foregoing results it can be concluded that providing a taper on the wall thickness of a boom can effectively reduce maximum bending stress, tip deflection and boom mass. It should be pointed out that the illustrated booms are of open section type and the analysis is based on the simple beam theory. Therefore, for overlapped STEM booms, the results are valid for small overlaps where the section stiffness does not change significantly due to twisting coupled with bending. For large overlaps, the results are valid only qualitatively. In the case of BI-STEMS, interfacial friction§ and end fixities allow very little relative

§ Interfacial friction in BI-STEM is obtained by making the outside diameter of inner element slightly larger than inside diameter of outer element before assembly.

movement of the two elements until near the bending failure loads. Therefore, a BI-STEM section acts almost as a rigid section and the above results are valid for design.

References

- ¹ Rimrott, F. P. J., "Storable Tubular Extendible Member—A Unique Machine Element," *Machine Design*, Vol. 37, No. 28, Dec. 1965, pp. 156–165.
- ² Herzl, G. G., "Tubular Spacecraft Booms (Extendible, Reel Stored)," *Aerospace Mechanism Series*, Vol. 2, Lockheed Missiles and Space Co., Sunnyvale, Calif., 1970.

Vortex-Induced Heating to a Cone-Cylinder Body at Mach 6

JERRY N. HEFNER*

NASA Langley Research Center, Hampton, Va.

RECENT experimental studies have shown that vortices can strongly influence heating on the leeward surface of conceptual hypersonic vehicles.^{1–6} The interaction of these vortices with the leeward surface creates relatively high shear regions in otherwise low shear or separated flow regions. Oil flow studies show that this high shear, which is created by the scrubbing action of the vortices on the surface, creates a featherlike oil smear. Comparisons of heat transfer data with oil flow studies show that the heating levels corresponding to the featherlike oil smears are elevated above the heating levels found in the areas adjacent to the oil smear. Previous studies on early design space shuttle orbiters^{1–3,6} have shown that the most severe vortex-induced lee-surface heating occurred in a region along the lee meridian where the interaction of the primary vortices with the lee surface created a relatively large, well defined featherlike oil smear. The present Note presents data on a blunt three-dimensional body which shows that the most severe vortex-induced lee-surface heating need not occur as a result of the interaction of the primary vortices with the lee surface even

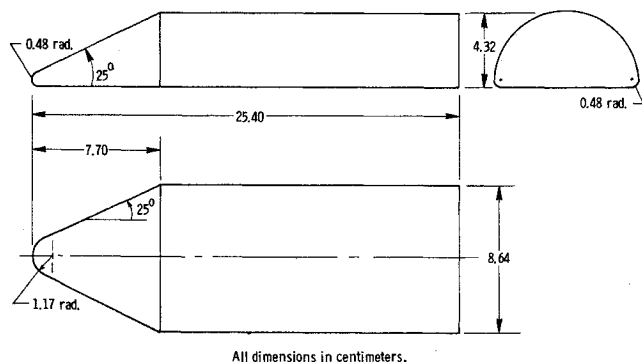


Fig. 1 Sketch of flat-bottom 25° half angle cone-cylinder model.

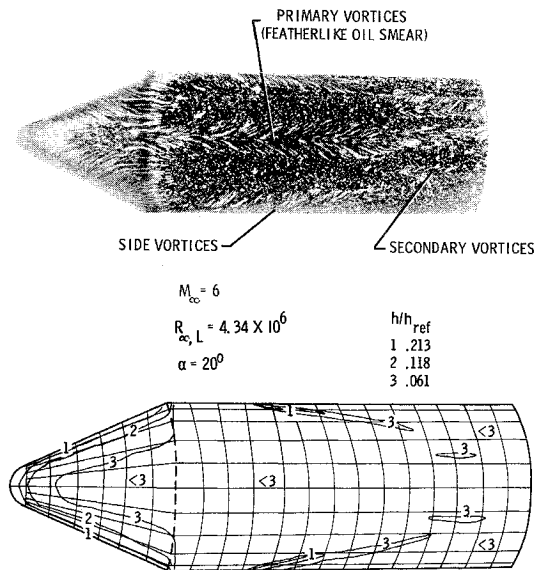


Fig. 2 Heat transfer and surface oil flow.

though this interaction produces a large, well defined featherlike oil smear.

Heat transfer and oil flow studies were conducted on a flat bottom 25° half angle cone-cylinder body at 20° angle of attack in the Langley 20 in. Mach 6 wind tunnel⁷ at a freestream Reynolds number based on model length ($R_{\infty, L}$) of 4.34×10^6 . A sketch of the model is presented in Fig. 1. The heat transfer data were obtained by using the phase-change paint technique⁸ with an assumed laminar recovery factor of 0.86 based on free-stream conditions. The measured local heat transfer coefficient (h) was normalized by the calculated stagnation heat transfer coefficient⁹ on a sphere having a 0.31 cm radius (h_{ref}). Oil flow studies were obtained by distributing a mixture of silicon oil and lampblack in random dots of varying sizes over the entire upper surface and taking photographs of the model after each test.

The oil flow photograph of Fig. 2 shows a highly complex lee-surface flow containing a number of vortices. The flow separating over the model forebody forms a primary vortex pair that interacts with the afterbody surface along the vertical plane of symmetry. Secondary vortices, which are smaller in size than the primary vortices, are formed outboard to either side of the primary vortices and interact with the afterbody lee surface. In addition to these primary and secondary vortices, side vortices, generated on the sides of the leeward afterbody at the abrupt change in planform area, also interact with the afterbody surface.

The secondary and side vortex-induced heating levels on the afterbody of the flat bottom cone-cylinder body are greater than was measured for the primary vortices even though the featherlike oil smear generated by the primary vortices was larger and much better defined than those generated by either the secondary or side vortices. This result is in contrast to that reported in Refs. 1–3 and 6 where the most severe vortex induced heating was generated by the primary vortices along the lee meridian. The heating due to the primary vortices in the present study is probably elevated above that found for the separated flow surrounding the feather pattern but was not measured for the present test times and phase-change paint temperature.

These results together with the work in Refs. 1–6 lead to the conclusion that the existence of a well defined featherlike oil smear generated along the lee meridian by the interaction of the primary lee side vortices with the surface does not necessarily indicate the region of the most severe vortex-induced heating. It should be remembered that Ref. 3 showed that the severity of vortex-induced heating is extremely sensitive to Reynolds

Received September 6, 1973; revision received October 4, 1973.

Index categories: Supersonic and Hypersonic Flow; LV/M Aerodynamic Heating.

* Aerospace Engineer, Analytical Fluid Mechanics Section, Hypersonic Vehicles Division. Member AIAA.